

Title	Effects of temporal laser profile on the emission spectra for underwater laser-induced breakdown spectroscopy: Study by short-interval double pulses with different pulse durations
Author(s)	Tamura, Ayaka; Matsumoto, Ayumu; Nakajima, Takashi; Fukami, Kazuhiro; Ogata, Yukio H.; Nishi, Naoya; Sakka, Tetsuo
Citation	Journal of Applied Physics (2015), 117(2)
Issue Date	2015-01-09
URL	http://hdl.handle.net/2433/196883
Right	© 2015 American Institute of Physics. This article may be downloaded for personal use only. Any other use requires prior permission of the author and the American Institute of Physics.
Type	Journal Article
Textversion	publisher

Effects of temporal laser profile on the emission spectra for underwater laser-induced breakdown spectroscopy: Study by short-interval double pulses with different pulse durations

Ayaka Tamura,^{1,a)} Ayumu Matsumoto,¹ Takashi Nakajima,² Kazuhiro Fukami,³
 Yukio H. Ogata,² Naoya Nishi,¹ and Tetsuo Sakka^{1,b)}

¹*Department of Energy and Hydrocarbon Chemistry, Graduate School of Engineering, Kyoto University, Kyoto 615-8510, Japan*

²*Institute of Advanced Energy, Kyoto University, Uji, Kyoto 611-0011, Japan*

³*Department of Materials Science and Engineering, Graduate School of Engineering, Kyoto University, Kyoto 606-8501, Japan*

(Received 24 October 2014; accepted 20 December 2014; published online 9 January 2015)

We investigate the effects of temporal laser profile on the emission spectra of laser ablation plasma in water. We use short-interval (76 ns) double pulses with different pulse durations of the composing two pulses for the irradiation of underwater target. Narrow atomic spectral lines in emission spectra are obtained by the irradiation, where the two pulses are wide enough to be merged into a single-pulse-like temporal profile, while deformed spectra are obtained when the two pulses are fully separated. The behavior of the atomic spectral lines for the different pulse durations is consistent with that of the temporal profiles of the optical emission intensities of the plasma. All these results suggest that continuous excitation of the plasma during the laser irradiation for ~ 100 ns is a key to obtain narrow emission spectral lines. © 2015 AIP Publishing LLC.

[<http://dx.doi.org/10.1063/1.4905392>]

I. INTRODUCTION

Laser-induced breakdown spectroscopy (LIBS) is based on the emission spectroscopy of laser ablation plasma, and can be applied to *in-situ* surface elemental analysis of solid targets in various environments.^{1–3} Especially, LIBS has a potential to be applied even to underwater environments, and the application to *in-situ* remote analysis at the bottom of the sea/lake is highly desired.^{4–11} However, the emission spectra of the laser-induced plasma in water are severely deformed^{12–14} due to the strong confinement effect on the plasma.^{15–17} To overcome this problem, double-pulse or multi-pulse irradiation with a pulse interval of tens of microseconds^{4,12,18–22} and single long-pulse (~ 150 ns) irradiation^{5,23–26} have been investigated, and the use of such irradiation schemes have been found to improve the spectral features of atomic lines for underwater LIBS applications, i.e., narrow spectral lines are obtained. In the case of single-pulse irradiation, we have reported in our previous paper²³ that the spectral line shape improves drastically with increasing laser pulse width, and the pulse width of ~ 150 ns gives narrow and intense spectral lines, sufficient for the application to underwater LIBS. In the case of a single short pulse with the pulse duration of several nanoseconds, however, spectral lines are severely deformed and their intensity is very low. Note that such a short pulse is readily obtained by commercial Q-switched Nd:YAG lasers and often employed in LIBS experiments. On the other hand, the laser-induced plasma in water is accompanied by a cavitation bubble,^{27–33} and it seems important to control the bubble as well for the

observation of narrow spectral lines. In conventional double-pulse or multi-pulse LIBS, we have to control the pulse interval so that the second pulse irradiates the target in a well-expanded bubble produced by the first pulse, and this pulse interval is usually several tens of microseconds.¹⁹ It has been clarified that the emission spectra obtained by the single-pulse LIBS are not affected by the hydrostatic pressure up to 30 MPa, i.e., narrow spectral lines are obtained even at high pressure up to 30 MPa by employing a long pulse as an irradiation laser.⁵ On the other hand, the conventional double-pulse scheme with a pulse interval of tens of microseconds is not suitable for high-pressure environments more than 5 MPa, because the bubble cannot expand to a certain volume.^{4,34} As a result, narrow spectral lines cannot be obtained at high pressure like 30 MPa by this scheme. Therefore, the long-pulse LIBS seems to be the best choice at present for the deep-sea investigations.

However, the long-pulse LIBS, in which typically ~ 100 to 150 ns laser pulse is used, has a problem in shot-to-shot stability, i.e., the spectral shape and the intensity of the LIBS signals seriously suffer from the shot-to-shot fluctuations. This is probably because the slow rise of the leading edge of the long pulse results in the timing of plasma generation varying shot-by-shot. On the other hand, short nanosecond pulse (typically ~ 5 to 20 ns), which is usually used in LIBS investigations, has a rapid rise of the leading edge, which means that the timing of the plasma generation with respect to the pulse peak is almost unchanged. If we could simulate the single long pulse with a combination of the short pulses without deteriorating the hydrostatic pressure effects and obtain the narrow spectral lines like those obtained by the single long pulse, the problem of the shot-to-shot fluctuation

^{a)}Electronic mail: tamura.ayaka.88m@st.kyoto-u.ac.jp

^{b)}Electronic mail: sakka.tetsuo.2a@kyoto-u.ac.jp

by the single long pulse would be solved. The simplest way to simulate the long pulse by using the short pulses is to use two short pulses with the pulse interval close to the pulse duration of the long pulse, namely, several tens of nanoseconds to ~ 100 ns. This new double-pulse LIBS with such a short pulse interval (~ 100 ns) is conceptually different from the conventional double-pulse LIBS with a pulse interval of tens of microseconds. While the latter aims at the ablation of the target in a rarefied gas provided by the well-expanded bubble, the former can be expected to directly excite the hot species ablated by the first pulse in an undeveloped bubble. It should be noted that double-pulse LIBS with such a short pulse interval has not been reported so far.

On the other hand, in the single long-pulse scheme, the leading edge of the long pulse (~ 150 ns) is known to ablate the target and produce the plasma,²⁶ while the mechanism to result in the well-defined spectral lines is not clear so far. It has been observed that the bubble expands to ~ 100 μm at the end of the long pulse,²⁶ and hence, later part of the long pulse interacts directly with the plasma in the bubble, which is in contrast to the case of short-pulse irradiation. In terms of simulating the long pulse with the short-interval double pulses, the second pulse of the double pulse should directly correspond to the later part of the long pulse. Since we can control the energy provided by the second pulse independently from the first pulse, which is simulating the earlier part of the long pulse, we should be able to assess the effects of the first and the second pulses separately by the short-interval double-pulse experiments, and hence, clarify the difference in the roles of the leading edge and the tailing edge of the long pulse. Therefore, the short-interval double-pulse experiments are expected to give important insight into the mechanism by which narrow spectral lines are obtained using the long-pulse LIBS.

In the present study, we investigate the effects of temporal laser profiles on the underwater LIBS spectra by using double pulses with a short pulse interval. More precisely, we fix the interval between the two pulses to be 76 ns and vary the durations of the two pulses from 30 to 100 ns. Since the two pulses have an identical temporal profile with similar pulse energies, a variation of the pulse duration results in the different temporal profiles of the irradiation laser, i.e., fully merged continuous pulse, slightly pitted merged pulse, and fully separated pulses in a single shot. We observe the emission spectra from the laser-ablated target after a certain delay from the laser pulse as well as the temporal variation of the total (spectrally integrated) optical emission from the plasma, and discuss the effects of the laser profiles on the ablation dynamics. We also discuss the behavior of the shock wave from the viewpoint of the effect of the laser profile upon the excitation of the plasma.

II. EXPERIMENTAL

Experimental setup for the measurement of emission spectra is shown in Fig. 1. A home-built flashlamp-pumped Q-switched Nd:YAG laser oscillating at the fundamental wavelength of 1064 nm was used. After the half-wave plate (HWP), the laser beam was split to two beams by the

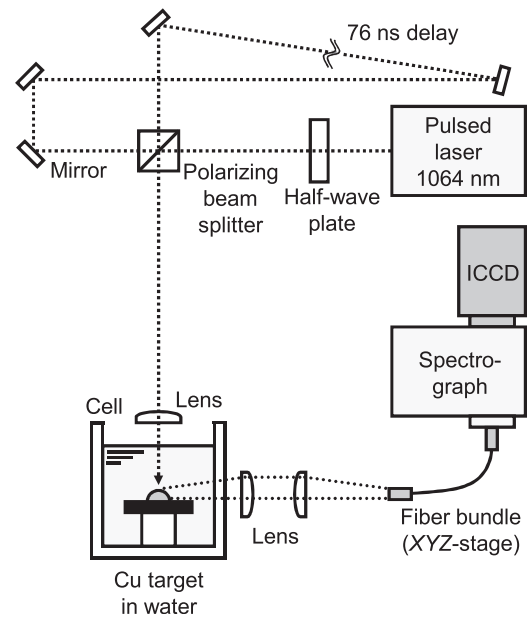


FIG. 1. Experimental setup for emission spectroscopy of laser ablation plasma in water with a short-interval double-pulse irradiation.

polarizing beam splitter (PBS). We prepared the short-interval double pulse by prolonging the optical path of one beam, and then combining the two beams again. The energies of the first and second pulses were 1.4 mJ and 0.9 mJ, respectively. The total energy was adjusted by adjusting the energy of the laser amplification, and the ratio between the energies of the first and second pulses was adjusted by the HWP. Although we have some pulse-to-pulse fluctuation of the pulse energy, the drift of the laser output is negligible within the time span of the experiment. After combining the two beams, we ensured the exact overlap of the two beams by measuring the spatial profile of the whole combined beam using a beam profiler (Thorlabs, BC106-VIS). The interval between the two pulses was set to 76 ns throughout this work. The repetition rate of the laser irradiation was 0.3 Hz. The pulse duration of the original pulse was controlled by the procedure given in our previous publication,²³ and was 30, 50, or 100 ns. The temporal profile of the laser was measured by detecting a portion of the beam reflected off by a glass plate. A fast silicon PIN photodiode was used as the detector. Note that the laser intensities obtained for different pulse widths cannot be compared in this experiment, since we cannot exactly reproduce the optical setup for the detection by PIN photodiode, although the shape of the temporal profile is reliable. The laser beam was focused onto a target surface in the direction normal to the surface by a 70 mm focal-length plano-convex lens. A Cu plate (Nilaco, CU-113421) used as a target was placed in a quartz cell filled with pure water (Millipore, Milli-Q). The plasma emission was focused into an optical fiber bundle (Oriol Instruments, 77 532) by two 60 mm focal-length plano-convex lenses. The direction of the observation was vertical to the laser propagation. The end of the fiber was connected to the spectrograph (Bunkoukeiki, MK-302) equipped with an intensified CCD (ICCD) (Princeton Instruments, ICCD-1024MTDGE/1). The slit width and the diffraction grating used in the spectrograph

are 100 μm and 1200 grooves/mm, respectively. The emission spectra were measured at the delay time of 1000 ns after the laser irradiation. The gate width of the ICCD was set to 1000 ns. The trigger level was set to the rising edge of the laser pulse. We observed spectral lines of Cu I 324.8 and 327.4 nm. Since the lower level for these lines is the ground state, the emission can be immediately re-absorbed by abundant ground state atoms, and therefore the spectral lines suffer from the strong self-absorption. Therefore, the choice of these spectral lines allows us a severe test for the effects upon the spectral deformation.

The shadowgraph images were measured by another ICCD (Roper Scientific, PI-MAX: 1K). A flashlamp (Morris, Hikorikomachi) was used as a back illumination light. A 10 \times microscope objective lens (Mitutoyo, M Plan Apo 10 \times) and an imaging lens (Mitutoyo, MT-4) were used as imaging optics. The shadowgraph images were observed at the delay time of 400 ns after the laser irradiation. The gate width of the ICCD was set to 5 ns.

The temporal profile of overall emission intensity was recorded using an avalanche photodiode (APD) (Hamamatsu Photonics, C5658) with nanosecond time-resolution. To avoid the detection of the scattering of Nd:YAG laser, four heat absorbing filters (OD3 at 1064 nm) (Hoya Candeo Optronics, HA30) were placed in front of the APD.

III. RESULTS AND DISCUSSION

In Fig. 2, an emission spectrum and a shadowgraph image obtained by the irradiation with a single long pulse are shown. The pulse energy and the pulse duration were 2.3 mJ and 100 ns, respectively. In the measurement of the emission spectrum, the delay time and the gate width of the ICCD were 1000 ns after the laser irradiation and 1000 ns, respectively. In the measurement of the shadowgraph image, the delay time and the gate width of the ICCD were 400 ns after the laser irradiation and 5 ns, respectively. Narrow spectral lines were obtained, and a shock wave was clearly observed.

Figure 3 shows the temporal profiles of the double pulse in the case of three different original pulse durations (30, 50,

and 100 ns), and emission spectra, shadowgraph images, and temporal profiles of the overall plasma emission intensity, corresponding to each temporal profile of the double pulse. As shown in Fig. 3(a), the pulse with a short duration results in a fully separated laser profile, while the pulse with a long duration at the same interpulse delay results in a laser profile in which two pulses are merged. In other words, by the different choices of time durations of double pulses, the laser profiles with fully merged pulse, with slightly pitted merged pulse, and with fully separated pulses were obtained.

Figure 3(b) shows the emission spectra of Cu I spectral lines obtained by the irradiation with double pulses having three different pulse durations (30, 50, and 100 ns) as shown in Fig. 3(a). Since the lower level for these emission lines is the ground state and hence highly populated, the spectral shape of the emission lines can be easily deformed by the self absorption effect.^{35,36} We selected these lines to sensitively detect the effects of the temporal laser profile on the spectral quality. It is clearly seen in Fig. 3(b) that the shape of the emission spectra varies considerably depending on the temporal profile of double pulses. For the individual pulse duration of 30 ns (fully separated double pulses), the emission spectrum is extremely broadened and seriously deformed, and a self-reversed structure appears. The intensity of the lines is low. For the individual pulse duration of 50 ns (slightly pitted merged double pulses), the deformation and the self-reversed structure seem to be slight. The self-reversed structure is caused by a temperature gradient along the detection line of the plasma as well as high density of the species involved in the transition.^{35,36} In addition to simple pulse-width effects, the experimental results in the present work indicate that the temporal variation of the laser pulse, i.e., a momentary decrease and subsequent increase of the laser intensity during the irradiation, causes the spectral deformation. For the individual pulse duration of 100 ns (fully merged double pulses), the narrow spectral lines without deformation are obtained, and the self-reversed structure is not seen. This means that the density of ablated species in the plasma is low and/or the temperature gradient of the plasma is smaller compared to that produced by the irradiation with

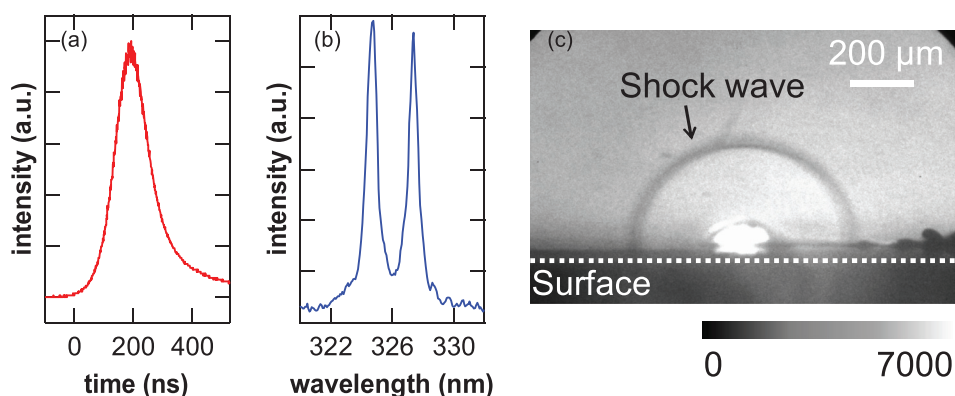


FIG. 2. (a) Temporal profile of a single long pulse, (b) emission spectrum, and (c) shadowgraph image. The results (b) and (c) were obtained by the irradiation of a Cu plate in water with the long-pulse laser, whose profile is depicted in the result (a). The pulse energy and the pulse duration were 2.3 mJ and 100 ns, respectively. For the measurement of the emission spectrum, the delay time and the gate width of the ICCD were 1000 ns after the laser irradiation and 1000 ns, respectively. For the measurement of the shadowgraph image, the delay time and the gate width of the ICCD were 200 ns after the laser irradiation and 5 ns, respectively.

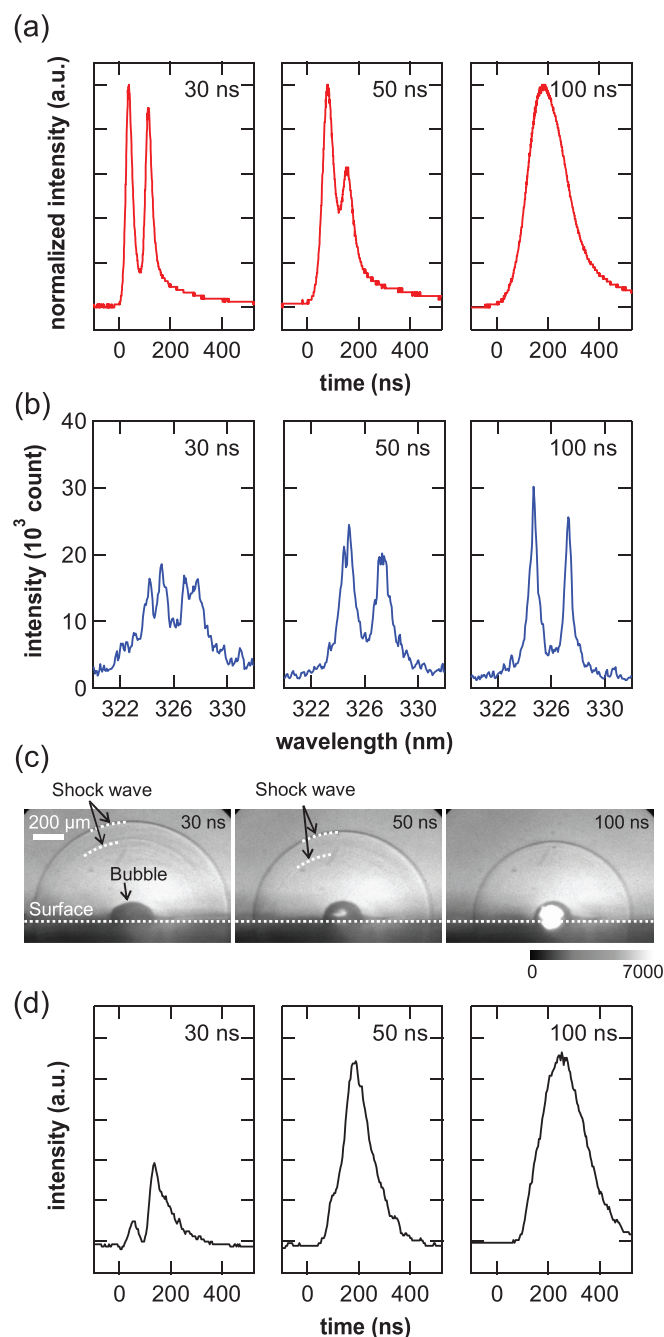


FIG. 3. (a) Temporal profiles of the double pulse with different original pulse durations, (b) emission spectra, (c) shadowgraph images, and (d) temporal profiles of the overall plasma emission intensity. The results (b)–(d) were obtained by the irradiation of a Cu plate in water with the double-pulse laser, whose profile is depicted in the result (a). The interval between the two pulses was 76 ns. The energies of the first and second pulses were 1.4 mJ and 0.9 mJ, respectively. The pulse durations of the individual pulses were 30 ns, 50 ns, and 100 ns. For the measurement of emission spectra, the delay time and the gate width of the ICCD were 1000 ns after the laser irradiation and 1000 ns, respectively. For the measurement of shadowgraph images, the delay time and the gate width of the ICCD were 400 ns after the laser irradiation and 5 ns, respectively.

fully separated double pulses, provided that the pulse energy is the same. The above findings in our double-pulse experiments at the same total pulse energy and pulse interval but with different pulse widths are consistent with the known facts that, if the pulse energy is kept to be the same, the use of a high-intensity or equivalently short laser pulse results in

the high shock-induced pressure³⁷ and more ablated species as well as denser plasma,³⁸ which leads to the severe deformation in the emission spectra due to the self-absorption effect.

To gain better insight into the effect of double pulses with short intervals on the ablation dynamics in water, we now look into the behavior of the shock wave. Note that the shock wave is generated by the laser-induced breakdown.³⁹ To understand the behavior of energy deposit into the irradiation spot, we took shadowgraph images of the shock waves at the timing of 400 ns after the rising edge of the laser pulse. Figure 3(c) shows the shadowgraph images of the shock waves obtained by the irradiation with the three different double pulses as shown in Fig. 3(a). Two distinct shock waves were generated by the fully separated and slightly pitted merged double pulses, if we look into the images of Fig. 3(c) carefully. The presence of the second shock wave implies that the shock wave can be formed by the second breakdown at the target surface or in the plasma generated by the first laser pulse. In contrast, the fully merged double pulses generated only one shock wave. These results indicate that the ablation process is different for different laser pulse profiles.

We can gain further insight into the differences of the plasma excitation mechanism by directly observing the temporal profile of spectrally integrated plasma emissions for different irradiation laser profiles. Figure 3(d) shows the temporal variation of the plasma emission detected by the APD with nanosecond time-resolution. Each result corresponds to the laser profile shown in Fig. 3(a). When the fully separated double pulses irradiate the target, the plasma emission decays before the second pulse. In contrast, when the fully merged double pulses were irradiated, the plasma emission does not decay during the laser irradiation. Our view of the roles of the second pulse in the heating process of the plasma and/or the target is as follows. If we have a dense plasma at the timing of the second pulse, it is the plasma rather than the target that is heated. On the other hand, if the plasma has already been quenched at the timing of the second pulse, it is the target rather than the plasma that is heated. We would like to emphasize that the former is favorable to obtain spectra with less self-absorption effect, since the plasma expansion is enhanced due to the further supply of the laser energy into the plasma, resulting in a less dense plasma at the timing of the spectral measurement.

To clarify the role of the second pulse, we performed another experiment in which the second pulse energy was increased from 0.9 mJ to 3.0 mJ, while keeping the first pulse energy to be 1.4 mJ. The duration of the individual pulse was 50 ns. Figure 4 shows the temporal profile of the double pulse, emission spectrum, and the shadowgraph image. In Fig. 4(a), one can see the momentary decrease is significantly small compared with that in Fig. 3(a) for 50 ns duration, because we increased the energy of the second pulse. Narrow atomic emission lines were obtained, and also, the clear second shock wave was observed.

Shock wave generation is based on the supersonic fluid motion by an abrupt energy deposition by the laser irradiation. The results shown in Figs. 3(a), 3(c), and 4 seem to suggest that the shock wave is generated at the timing when the

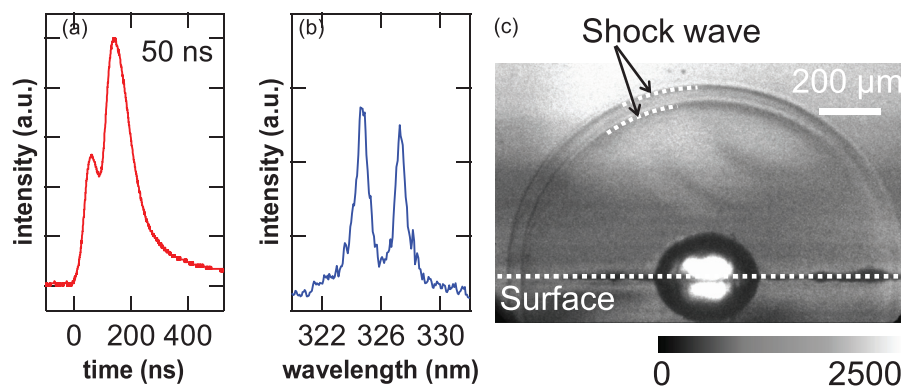


FIG. 4. (a) Temporal profile of the double pulse, (b) emission spectrum, and (c) shadowgraph image. The results (b) and (c) were obtained by the irradiation of a Cu plate in water with the double-pulse laser, whose profile is depicted in the result (a). The interval between the two pulses was 76 ns. The energies of the first and second pulses were 1.4 mJ and 3.0 mJ, respectively. The pulse duration of the individual pulse was 50 ns. For the measurement of emission spectrum, the delay time and the gate width of the ICCD were 1200 ns after the laser irradiation and 1000 ns, respectively. For the measurement of shadowgraph image, the delay time and the gate width of the ICCD were 400 ns after the laser irradiation and 5 ns, respectively.

temporal laser profile shows a rapid increase, and the presence of the plasma at this timing does not matter for the formation of the shock wave. The second shock wave is clearly seen in Fig. 4, while the optical emission from the plasma is expected to be still quite intense at the timing of the second pulse, which is suggested by the temporal profile of the plasma emission shown in the middle panel of Fig. 3(d). This suggests that the second pulse induces the breakdown under the presence of the plasma. The observation of the shock wave is interpreted as an abrupt energy deposition, but we cannot specify either the plasma or the surface to which the energy of the second pulse is directly deposited.

Observation of the narrow emission lines does not necessarily mean that the shock wave is not generated by the second pulse. Maintaining the plasma during the entire laser irradiation is rather essential to obtain the narrow emission lines. Although the second pulse supplies the same pulse energy in the experiments with different pulse durations shown in Fig. 3(a), the resultant optical emission spectra considerably depend on the duration of the individual pulse (Fig. 3(b)). It seems that a continuous supply of the laser energy without an interruption is favorable to obtain thin and sustainable plasma, leading to the narrow spectral lines and intense emission (see Figs. 3(b) and 3(d)). In the rising edge of the plasma emission profile for the case of 50 ns in Fig. 3(d), we can see a rapid rise of the intensity first, and then a small plateau-like structure followed by a rapid rise again. The timing of the second rise corresponds to the timing of the second pulse irradiation and the rapid energy deposition to the plasma could cause the second shock wave as we can see it, although not very clear, in Fig. 3(c), in the case of the pulse duration of 50 ns.

Consequently, in the case of a long-pulse irradiation the plasma generated at the leading edge of the long pulse is continuously absorbing the laser energy during the pulse to fulfill relatively low-atomic-density condition, which is suitable for underwater LIBS measurements. We would like to emphasize that the important point is not to control the total energy deposited to the irradiation spot during ~ 100 ns, but to continuously heat the plasma rather than the target surface for ~ 100 ns. In addition, in the single long-pulse LIBS, the

bubble expansion at the timing of spectral measurements is not affected by the external pressure.^{40,41} This leads to the conclusion that the temporal duration of the irradiation laser for underwater LIBS under high pressure should be long. However, this does not necessarily mean that single long-pulse irradiation is the best because it gives quite a large shot-to-shot fluctuation due to the slow rise of the leading edge. The present results show that the rapid rise of the laser profile does not deteriorate the spectral feature of the LIBS signal, as long as the plasma is continuously excited during the laser irradiation of ~ 100 ns. Therefore, by employing the combination of a short first pulse and a long second pulse, we expect narrow spectral lines like those obtained by a single long pulse, and at the same time, a lowered shot-to-shot fluctuation due to the stable plasma initiation with the first pulse being sufficiently short.

IV. CONCLUSIONS

In the present study, we have investigated the effects of the temporal laser profile of the short-interval (76 ns) double pulses on the spectral shapes of the underwater LIBS signal, i.e., emission spectra of the laser-ablated species from the target submerged in water. To control the temporal laser profile, we have employed double pulses with different durations (30, 50, and 100 ns) of individual pulses. If the individual pulse duration is long, the temporal laser profile of the double pulses is fully merged into a single long pulse, and the corresponding emission spectra exhibit sharp peaks, which is very favorable for the elemental analysis of the target in water. If, however, the individual pulse duration is short, the corresponding emission spectra are deformed. We have clarified that the above difference originates from the different dynamics of plasma to absorb laser energy. The key to obtain narrow emission lines suitable for underwater LIBS is to continuously supply energy into the plasma, rather than the target surface, by the laser with a duration of ~ 100 ns or longer. The generation of the second shock wave is not directly related to the observation of the narrow spectral lines. However, if the plasma is extinguished at the timing of the second pulse, the shock wave is generated by the ablation

of the target surface, and in this case we always observe the deformed spectra. Our findings suggest that the short-interval double pulses composed of the short first pulse and the long second pulse would be the optimal choice, where the stable initiation of the plasma is expected by the first short pulse and the narrow spectral lines are expected by the continuous energy supply into the plasma by the second long pulse.

ACKNOWLEDGMENTS

The authors thank Yu Qin for his contribution at the earlier stage of this work. This work was supported by JSPS KAKENHI Grant Nos. 23560023 and 13J04184.

- ¹D. A. Cremers and L. J. Radziemski, *Handbook of Laser-Induced Breakdown Spectroscopy* (John Wiley & Sons, Chichester, 2006).
- ²*Laser-Induced Breakdown Spectroscopy, Fundamentals and Applications*, edited by A. W. Miziolek, V. Palleschi, and I. Schechter (Cambridge University Press, Cambridge, 2006).
- ³F. J. Fortes, J. Moros, P. Lucena, L. M. Cabalín, and J. J. Laserna, *Anal. Chem.* **85**, 640 (2013).
- ⁴T. Takahashi, B. Thornton, and T. Ura, *Appl. Phys. Express* **6**, 042403 (2013).
- ⁵B. Thornton, T. Sakka, T. Takahashi, A. Tamura, T. Masamura, and A. Matsumoto, *Appl. Phys. Express* **6**, 082401 (2013).
- ⁶S. Guirado, F. J. Fortes, V. Lazic, and J. J. Laserna, *Spectrochim. Acta, Part B* **74**, 137 (2012).
- ⁷B. Thornton, T. Takahashi, T. Sato, T. Sakka, A. Tamura, A. Matsumoto, T. Nozaki, T. Ohki, and K. Ohki, *Deep-Sea Res., Part I* **95**, 20 (2015).
- ⁸A. P. M. Michel and A. D. Chave, *Appl. Opt.* **47**, G122 (2008).
- ⁹A. P. M. Michel and A. D. Chave, *Appl. Opt.* **47**, G131 (2008).
- ¹⁰M. Lawrence-Snyder, J. Scaffidi, S. M. Angel, A. P. M. Michel, and A. D. Chave, *Appl. Spectrosc.* **60**, 786 (2006).
- ¹¹M. Lawrence-Snyder, J. Scaffidi, S. M. Angel, A. P. M. Michel, and A. D. Chave, *Appl. Spectrosc.* **61**, 171 (2007).
- ¹²A. De Giacomo, M. Dell'Aglio, O. De Pascale, and M. Capitelli, *Spectrochim. Acta, Part B* **62**, 721 (2007).
- ¹³T. Sakka, S. Iwanaga, Y. H. Ogata, A. Matsunawa, and T. Takemoto, *J. Chem. Phys.* **112**, 8645 (2000).
- ¹⁴A. De Giacomo, M. Dell'Aglio, F. Colao, R. Fantoni, and V. Lazic, *Appl. Surf. Sci.* **247**, 157 (2005).
- ¹⁵K. Saito, K. Takatani, T. Sakka, and Y. H. Ogata, *Appl. Surf. Sci.* **197–198**, 56 (2002).
- ¹⁶T. T. P. Nguyen, R. Tanabe, and Y. Ito, *Appl. Phys. Lett.* **102**, 124103 (2013).
- ¹⁷N. Takada, T. Nakano, and K. Sasaki, *Appl. Surf. Sci.* **255**, 9572 (2009).
- ¹⁸R. Nyga and W. Neu, *Opt. Lett.* **18**, 747 (1993).
- ¹⁹A. E. Pichahchy, D. A. Cremers, and M. J. Ferris, *Spectrochim. Acta, Part B* **52**, 25 (1997).
- ²⁰V. Lazic, F. Colao, R. Fantoni, and V. Spizzicchio, *Spectrochim. Acta, Part B* **60**, 1014 (2005).
- ²¹T. Sakka, A. Tamura, T. Nakajima, K. Fukami, and Y. H. Ogata, *J. Chem. Phys.* **136**, 174201 (2012).
- ²²A. Tamura, T. Sakka, K. Fukami, and Y. H. Ogata, *Appl. Phys. A* **112**, 209 (2013).
- ²³T. Sakka, H. Oguchi, S. Masai, K. Hirata, Y. H. Ogata, M. Saeki, and H. Ohba, *Appl. Phys. Lett.* **88**, 061120 (2006).
- ²⁴H. Oguchi, T. Sakka, and Y. H. Ogata, *J. Appl. Phys.* **102**, 023306 (2007).
- ²⁵A. Matsumoto, A. Tamura, K. Fukami, Y. H. Ogata, and T. Sakka, *Anal. Chem.* **85**, 3807 (2013).
- ²⁶T. Sakka, A. Tamura, A. Matsumoto, K. Fukami, N. Nishi, and B. Thornton, *Spectrochim. Acta, Part B* **97**, 94 (2014).
- ²⁷V. Lazic, S. Jovicevic, and M. Carpanese, *Appl. Phys. Lett.* **101**, 054101 (2012).
- ²⁸T. Tsuji, Y. Okazaki, Y. Tsuboi, and M. Tsuji, *Jpn. J. Appl. Phys., Part 1* **46**, 1533 (2007).
- ²⁹Y. Kawaguchi, X. Ding, A. Narazaki, T. Sato, and H. Niino, *Appl. Phys. A* **80**, 275 (2005).
- ³⁰Y. Kawaguchi, X. Ding, A. Narazaki, T. Sato, and H. Niino, *Appl. Phys. A* **79**, 883 (2004).
- ³¹T. Tsuji, Y. Tsuboi, N. Kitamura, and M. Tsuji, *Appl. Surf. Sci.* **229**, 365 (2004).
- ³²K. Sasaki, T. Nakano, W. Soliman, and N. Takada, *Appl. Phys. Express* **2**, 046501 (2009).
- ³³W. Soliman, T. Nakano, N. Takada, and K. Sasaki, *Jpn. J. Appl. Phys.* **49**, 116202 (2010).
- ³⁴A. De Giacomo, A. De Bonis, M. Dell'Aglio, O. De Pascale, R. Gaudiuso, S. Orlando, A. Santagata, G. S. Senesi, F. Taccogna, and R. Teghil, *J. Phys. Chem. C* **115**, 5123 (2011).
- ³⁵R. D. Cowan and G. H. Dieke, *Rev. Mod. Phys.* **20**, 418 (1948).
- ³⁶T. Sakka, T. Nakajima, and Y. H. Ogata, *J. Appl. Phys.* **92**, 2296 (2002).
- ³⁷R. Fabbro, J. Fournier, P. Ballard, D. Devaux, and J. Virmont, *J. Appl. Phys.* **68**, 775 (1990).
- ³⁸T. Sakka, S. Masai, K. Fukami, and Y. H. Ogata, *Spectrochim. Acta, Part B* **64**, 981 (2009).
- ³⁹R. Petkovšek and P. Gregorčič, *J. Appl. Phys.* **102**, 044909 (2007).
- ⁴⁰B. Thornton, T. Sakka, T. Masamura, A. Tamura, T. Takahashi, and A. Matsumoto, *Spectrochim. Acta, Part B* **97**, 7 (2014).
- ⁴¹B. Thornton, T. Takahashi, T. Ura, and T. Sakka, *Appl. Phys. Express* **5**, 102402 (2012).